Entanglement Growth from Entangled States: A Unified Perspective on Entanglement Generation and Transport

Chun-Yue Zhang,[1,2] Zi-Xiang Li,[1,2,*] and Shi-Xin Zhang[1,†]
[1]*Beijing National Laboratory for Condensed Matter Physics and Institute of Physics, Chinese Academy of Sciences, Beijing 100190, China*
[2]*University of Chinese Academy of Sciences, Beijing 100049, China*

(Received 3 December 2025; revised 20 March 2026; accepted 2 June 2026; published 7 July 2026)

Studies of entanglement dynamics in quantum many-body systems have focused largely on initial product states. Here, we investigate the far richer dynamics from initial entangled states, uncovering universal patterns across diverse systems ranging from many-body localization (MBL) to random quantum circuits. Our central finding is that the growth of entanglement entropy can exhibit a counterintuitive nonmonotonic dependence on the initial entanglement in many nonergodic systems, peaking for moderately entangled initial states. To understand this phenomenon, we introduce a conceptual framework that decomposes entanglement growth into two mechanisms: "build" and "move." The "build" mechanism creates new entanglement, while the "move" mechanism redistributes preexisting entanglement throughout the system. Specifically, we demonstrate that MBL dynamics are "move-dominated," exhibiting a quantitative agreement with a random SWAP circuit that serves as a model of pure "move" dynamics by uniformly distributing preexisting entanglement. This implies that MBL acts as a redistributor of a hidden entanglement reservoir quantified by the bipartition-averaged entropy. This "build-move" framework offers a unified perspective for classifying diverse physical dynamics, deepening our understanding of entanglement propagation and information processing in quantum many-body systems.

DOI: 10.1103/xkh7-gdqm

Introduction—Entanglement is a cornerstone of modern physics [1–3] and specifically a key diagnostic for nonequilibrium quantum dynamics [4–10]. The standard approach investigates the time evolution of entanglement entropy (EE) from an initial product state, revealing a rich landscape of dynamical behaviors. In thermalizing systems and generic random quantum circuits (RQCs), entanglement grows rapidly, often linearly in time [11–26]. By contrast, many-body localized (MBL) systems [27–63] exhibit a much slower, logarithmic growth [64–72], while integrable systems saturate to nonthermal values [73–77] and noninteracting Anderson localized (AL) systems show severely suppressed entanglement growth [78–90]. However, this fruitful paradigm inherently conflates two distinct aspects of entanglement dynamics: the initial generation of entangled resources and the subsequent transport of this entanglement. The observed half-chain entanglement entropy (HCEE) growth is thus always a composite effect, leaving the underlying pattern of entanglement propagation obscured.

To deconstruct this process and isolate the intrinsic entanglement handling capabilities of a given system, we shift the paradigm to study the evolution of initial states that already possess volume-law entanglement, which we term partially thermalized states. These states are thus prepared to contain a rich, preexisting reservoir of entanglement, providing a nontrivial substrate for the subsequent dynamics. This paradigm shift allows us to move from the question "How fast is entanglement created?" to a more profound one: "How does a system's inherent dynamics process and redistribute preexisting entanglement?" This setup facilitates a deep probe into the intricate interplay between a system's fundamental character and an existing, complex entanglement structure.

In this Letter, we address these questions and uncover a remarkable phenomenon: in MBL dynamics, the HCEE growth exhibits a nonmonotonic behavior with its initial value, profoundly differing from thermalized systems [see Fig. 1(d)]. To rationalize the observed behaviors, we introduce a novel conceptual framework that decomposes HCEE growth into two primary mechanisms: "build" for creating new entanglement and "move" for redistributing preexisting entanglement, as schematically shown in Figs. 1(a) and 1(b), respectively. We demonstrate that this framework not only quantitatively explains our results by identifying MBL as a "move-dominated" dynamics but also provides a unified perspective for classifying diverse quantum dynamics.

Model and methods—We study the dynamics in a one-dimensional spin-$1/2$ chain of even length L using exact diagonalization. The central quantity of interest is the

[*]Contact author: zixiangli@iphy.ac.cn
[†]Contact author: shixinzhang@iphy.ac.cn

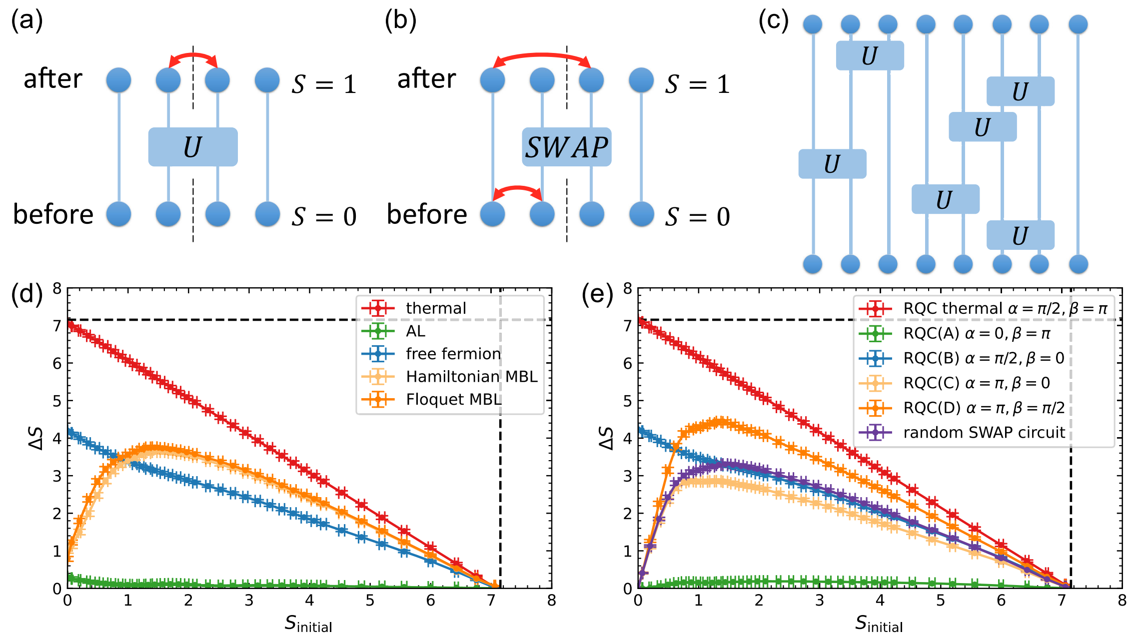

FIG. 1. "Build-move" framework and the increase of HCEE in various dynamics. (a)–(c) Schematic illustrations of "build" mechanism (a), "move" mechanism (b), and RQC composed of two-qubit gates U (c). Blue circles represent spins, and pairs of spins linked by red double arrows indicate Bell pairs. (d),(e) Classification of dynamics based on the HCEE growth: $\Delta S = S_{\rm sat} - S_{\rm initial}$ as a function of the initial HCEE, $S_{\rm initial}$. All data points are for system size $L = 16$. $S_{\rm initial}$ is controlled by varying the preparation time τ. (d) Results for Hamiltonian-based dynamics. (e) Results for RQC-based dynamics. Note the striking similarity between the MBL curve in (d) and the Random SWAP curve in (e). The two-qubit gates U are defined in Eq. (2), with parameters in various classes detailed in Table I. For the calculation details of the data in all figures in the main text, please refer to Supplemental Material, Sec. I [91].

HCEE measured in bits: $S = -\mathrm{Tr}(\hat{\rho}_{\rm HC}\log_2\hat{\rho}_{\rm HC})$, defined as the von Neumann entropy of the first $L/2$ spins whose reduced density operator is $\hat{\rho}_{\rm HC}$. The various physical processes in our study, from initial state preparation to subsequent dynamics, are mainly based on the one-dimensional disordered XXZ Hamiltonian with open boundary conditions:

$$\hat{H} = \sum_{i=1}^{L-1}\left(\hat{S}_i^x\hat{S}_{i+1}^x + \hat{S}_i^y\hat{S}_{i+1}^y + J_z\hat{S}_i^z\hat{S}_{i+1}^z\right) + \sum_{i=1}^{L} h_i\hat{S}_i^z. \quad (1)$$

Here, $\hat{S}_i^\alpha$ ($\alpha = x, y, z$) are the spin-1/2 operators at site i, and we set the anisotropy $J_z = 0.5$. The on-site fields h_i are independent random variables drawn uniformly from the interval $[-W, W]$. This Hamiltonian has a $U(1)$ symmetry which conserves the total magnetization in the z direction, $\hat{S}^z_{\rm tot} = \sum_{i=1}^{L}\hat{S}_i^z$. All calculations are performed in the half-filling sector $\hat{S}^z_{\rm tot} = 0$. The system is in the thermal and MBL phases at $W = 0.5$ and $W = 5.0$, respectively [29] [see Supplemental Material (SM), Sec. II [91] for details].

Our primary focus is on the evolution from initial states with varying degrees of entanglement. We prepare initial states $|\psi(\tau)\rangle$ by evolving a product state $|\psi_0\rangle$ under the thermal Hamiltonian $\hat{H}(W = 0.5)$ for a duration τ. $|\psi_0\rangle$ is randomly chosen from the computational basis states within the half-filling sector. The evolution time τ directly controls the initial entanglement and the level of thermalization as $|\psi(\tau)\rangle = \mathrm{e}^{-\mathrm{i}\tau\hat{H}(W=0.5)}|\psi_0\rangle$. Subsequently, we examine the dynamics of these prepared states under the following $U(1)$-symmetric dynamical protocols: (1) Thermal dynamics: $|\psi(\tau)\rangle$ evolves under the thermal Hamiltonian $\hat{H}(W = 0.5)$. (2) Hamiltonian MBL dynamics: $|\psi(\tau)\rangle$ evolves under the MBL Hamiltonian $\hat{H}(W = 5.0)$. (3) Free fermion dynamics: evolution under the free fermion Hamiltonian $\hat{H}_{\rm XY}$ with $J_z = 0$ and $W = 0$ in Eq. (1). (4) Floquet MBL dynamics: a periodic drive is applied using the Floquet operator $\hat{F} = \mathrm{e}^{-\mathrm{i}T_0\hat{H}_0}\mathrm{e}^{-\mathrm{i}T_1\hat{H}_{\rm XY}}$ [57]. Here, $\hat{H}_0 = \sum_{i=1}^{L-1}\hat{S}_i^z\hat{S}_{i+1}^z + \sum_{i=1}^{L}h_i\hat{S}_i^z$, with disorder strength $W = 5.0$, $T_0 = 1.0$, and $T_1 = 0.4$. (5) AL dynamics: $|\psi(\tau)\rangle$ evolves under the noninteracting AL Hamiltonian, with $J_z = 0$ and $W = 5.0$ in Eq. (1). (6) RQC protocols: we employ RQCs as a paradigmatic model for understanding universal aspects of entanglement dynamics [15,17,22,23,102–114]. Our implementation consists of circuits where, at each step, a single two-qubit gate U is applied to a randomly selected adjacent pair of spins $(i, i+1)$ from the $L-1$ bonds [Fig. 1(c)]. The two-qubit unitary is given by

$$\hat{U}_{i,i+1} = \mathrm{e}^{-\mathrm{i}\alpha\left(\hat{S}_i^x\hat{S}_{i+1}^x + \hat{S}_i^y\hat{S}_{i+1}^y\right)}\mathrm{e}^{-\mathrm{i}\beta\hat{S}_i^z\hat{S}_{i+1}^z}. \quad (2)$$

Results—To analyze the entanglement dynamics under different protocols, we first introduce a conceptual framework that decomposes the growth of HCEE into two fundamental mechanisms: "build" and "move." As shown in Fig. 1(a), the "build" mechanism creates new entanglement directly. For instance, a two-qubit unitary gate U across the central bond can generate a Bell pair from a product state, increasing the HCEE from 0 to 1. The "move" mechanism, depicted in Fig. 1(b), involves the redistribution of preexisting entanglement. Here, an entangled pair within one subsystem is transported across the central bond, for instance, via a SWAP gate, also raising HCEE from 0 to 1. While both mechanisms often occur simultaneously in a generic interacting system, their proportional contributions are highly dependent on the specific dynamics.

To isolate the "move" mechanism, we employ the random SWAP circuit as an idealized model, which can be achieved up to a global phase by setting $\alpha = \beta = \pi$ in our RQC protocols. The key insight is that a SWAP operation merely exchanges the state of two spins. This allows us to equivalently view the action of the random SWAP circuit on a fixed bipartition as an evolution of the bipartition itself across a static state. This evolution generates transitions between the $N = \binom{L}{L/2}/2$ distinct bipartitions, establishing an ergodic Markov chain with a uniform stationary distribution (see the proof in SM, Sec. III [91]). Consequently, at sufficiently large circuit depth, every bipartition becomes equally probable. This directly implies that the steady-state HCEE under the random SWAP circuit corresponds precisely to the initial state's *bipartition-averaged entanglement entropy* (BAEE)—the entanglement entropy averaged across all N possible equal-size bipartitions: $\bar{S} = (1/N) \sum_{A \in \mathcal{P}} S_A$, where $\mathcal{P}$ is the set consisting of subsystems corresponding to all N possible bipartitions and S_A represents the entropy of the subsystem A on $\mathcal{P}$. The BAEE provides a more robust measure of the state's overall entanglement, invariant under SWAP dynamics, which only redistributes existing entanglement. This model thus establishes a baseline for move-driven dynamics, enabling quantitative comparisons with more complex protocols. For more analysis about the BAEE, see SM, Sec. VI [91].

For RQC protocols of $\alpha, \beta \in [0, 2\pi]$, the specific points $(\alpha, \beta) = (0, 0), (0, 2\pi), (2\pi, 0)$, and $(2\pi, 2\pi)$ are trivial as the operator $\hat{U}_{i,i+1}$ can be decomposed into a tensor product of single-qubit gates. Generic choices of (α, β) are expected to lead to full thermalization, where the HCEE saturates near the Haar measure average value in the half-filling sector [115–119], which is marked by dashed lines in Figs. 1(d), 1(e), 2, and 3. Nonthermalization behavior occurs only for a small set of special parameter values, which we classify into five categories based on the distinct saturation values of their HCEE. Within each category, different parameter choices for (α, β) lead to dynamics with almost the same saturating HCEE value. The random SWAP circuit mentioned above is one of these five

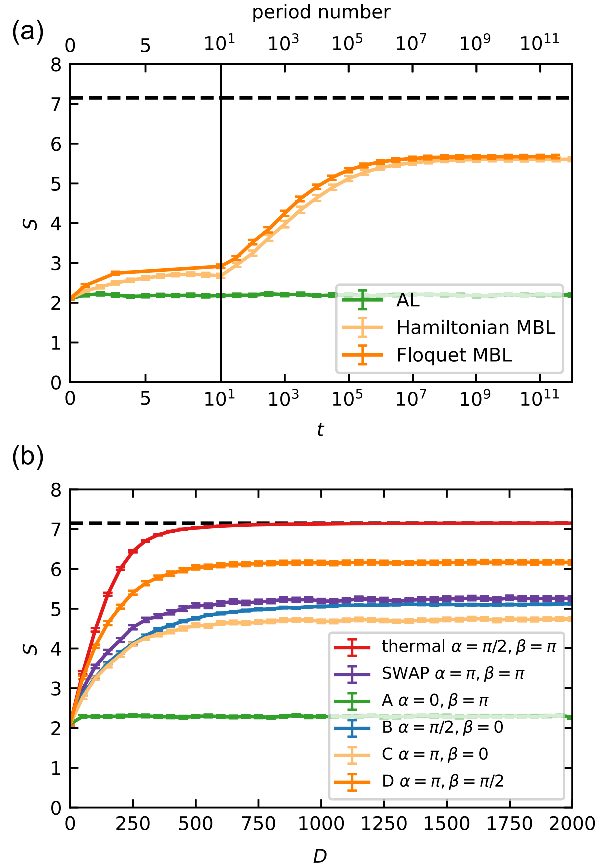

FIG. 2. Time evolution of HCEE S with initial state $|\psi(\tau)\rangle$ for $L = 16$ and $\tau = 4.5$. (a) Evolution under localized dynamics. The lower axis shows time t for AL and Hamiltonian MBL evolutions, and the upper axis shows the period number for the Floquet MBL dynamics. To visualize the dynamics across multiple timescales, the horizontal axis uses a hybrid scale of linear time for the initial evolution (t, period number < 10) and logarithmic for long times. (b) Evolution under RQCs dynamics. The horizontal axis represents the circuit depth. The specific (α, β) values shown in the legend are the parameters of the quantum gates selected from their respective categories.

categories. The parameter setting for these categories is summarized in Table I.

Figure 2(a) displays the localized dynamics for a long time starting from $|\psi(\tau)\rangle$, where the evolution under different nonthermal dynamics reveals distinct behaviors. For both the Hamiltonian MBL and the Floquet MBL protocols, the HCEE exhibits a characteristic slow, logarithmic growth in time. It eventually reaches a saturation value that, while significantly higher than the initial HCEE, remains well below the Haar measure average value in the half-filling sector. In sharp contrast, the dynamics governed by the noninteracting AL Hamiltonian [Fig. 2(a)] and the RQC(A) protocol [Fig. 2(b)] both show almost no further increase in HCEE, among which the former confirms that interactions are crucial for moving the entanglement.

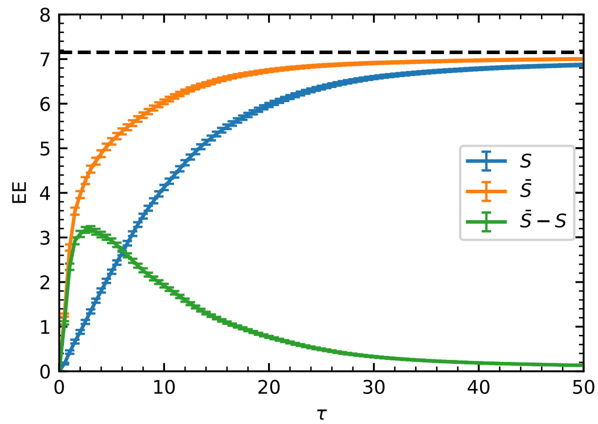

FIG. 3. Evolution of BAEE $\bar{S}$, HCEE S, and their difference under thermal Hamiltonian $\hat{H}(W = 0.5)$ for $L = 16$, starting from the product state $|\psi_0\rangle$. The data point corresponding to the maximum value of $\bar{S} - S$ is at $\tau = 3.0$ with HCEE $S \approx 1.34$, roughly coinciding with the optimal S_{initial} for the peak ΔS of move-dominated dynamics in Figs. 1(d) and 1(e).

The other nonthermal RQC protocols, RQC(B)–(D), all facilitate HCEE growth, but with distinct steady values.

To systematically quantify the relationship between initial entanglement and subsequent entanglement growth, we analyze the total increase of HCEE, $\Delta S = S_{\mathrm{sat}} - S_{\mathrm{initial}}$, as a function of S_{initial}. The results, plotted in Figs. 1(d) and 1(e), reveal that the diverse dynamical protocols can be classified into three classes based on their monotonicity, which reflects the capability to generate and transport entanglement. This classification not only is supported by the macroscopic behavior of ΔS but also is consistent with the microscopic action of the gate for the RQC dynamics.

Move-dominated dynamics—The first class of protocols is defined by a predominant "move" mechanism, whose fundamental role is to redistribute existing entanglement. As depicted in Fig. 1(d), the dynamics of MBL clearly exhibit a nonmonotonic dependence of ΔS on S_{initial}. This behavior, which differs significantly from that in thermal or AL dynamics, is a key finding of this Letter. For nearly product states ($S_{\mathrm{initial}} \approx 0$), ΔS is negligible due to the minimal entanglement available for transport. It then increases to a peak for moderately entangled states before decreasing again as S_{sat} approaches the Haar measure average value. This distinct nonmonotonic behavior serves as a hallmark of the move-dominated mechanism. More importantly, we find the quantitative agreement of the results from MBL and random SWAP circuits, although the time scales for entanglement saturation are distinct for these dynamics. This agreement is highly nontrivial: it implies that, despite the complex Hamiltonian origin of MBL, its effective entanglement dynamics approximately reduces to a simple shuffling of bipartitions. This class also encompasses RQC(C) and (D), as illustrated in Fig. 1(e). This is directly explained by their gate-level action, which functions similarly to a SWAP operator. For example, when an RQC(C) or (D) gate acts on the first two spins of the state $|\uparrow\uparrow\downarrow\rangle + |\uparrow\downarrow\uparrow\rangle$, the transformation yields $\mathrm{e}^{-\mathrm{i}\beta/4}|\uparrow\uparrow\downarrow\rangle - \mathrm{i}\mathrm{e}^{\mathrm{i}\beta/4}|\downarrow\uparrow\uparrow\rangle$. This effectively converts entanglement from between the last two spins to between the first and third spins, thereby realizing the "move" operation at the microscopic level.

Build and move hybrid dynamics—The second class of dynamics exhibits a hybrid "build-and-move" character. In conventional thermal systems, a significant ΔS emerges even from initial product states ($S_{\mathrm{initial}} = 0$), signifying the "build" mechanism that generates entanglement from scratch [Fig. 1(d)]. This entanglement increase, ΔS, diminishes as S_{initial} rises. Similarly, free fermion systems also reach the equilibrium with weaker "build" capabilities due to extensive conserved quantities, resulting in a smaller ΔS. Consistent with this, RQCs with general $\alpha \in (0, \pi) \cup (\pi, 2\pi)$, including both thermal RQC and RQC(B), also show the same monotonically decreasing trend of ΔS, as shown in Fig. 1(e). The ability of these RQCs to effectively generate entanglement from product states—for instance, transforming $|\uparrow\downarrow\rangle$ into the entangled state $\mathrm{e}^{\mathrm{i}\beta/4}[\cos(\alpha/2)|\uparrow\downarrow\rangle - \mathrm{i}\sin(\alpha/2)|\downarrow\uparrow\rangle)$, further corroborates the pervasive "build" mechanism within this class. Specifically, RQC(B) with $\beta = 0$ mimics free fermion dynamics. Moreover, with increasing S_{initial}, the "move" aspect for these systems also becomes a prominent contributor to the overall entanglement growth.

Entanglement-inert dynamics—Finally, the third class is essentially inert with respect to HCEE growth. Both AL and RQC(A) fall into this class, producing negligible ΔS across the entire range of S_{initial} [see Figs. 1(d) and 1(e)]. This inert behavior stems from the lack of essential ingredients for either "build" or "move" contribution. For AL, the noninteracting and localized character of the Hamiltonian prevents entanglement from forming or

TABLE I. Classification of Hamiltonian-based and RQC-based dynamics on the behavior of ΔS with S_{initial}.

Hamiltonian-based dynamics	RQC-based dynamics	Tendency of ΔS with S_{initial}
Thermalization	$\alpha \in (0, \pi) \cup (\pi, 2\pi)$, $\beta \in (0, 2\pi)$	Monotonic decay
MBL	$\alpha = \pi, \beta = \pi$ (SWAP), $\{0, 2\pi\}$ (class C), other values (class D)	Nonmonotonic peak
Free fermion	$\alpha \in (0, \pi) \cup (\pi, 2\pi)$, $\beta = \{0, 2\pi\}$ (class B)	Monotonic decay
AL	$\alpha = \{0, 2\pi\}$, $\beta \in (0, 2\pi)$ (class A)	Negligible

spreading. For RQC(A), the underlying gate is diagonal in the computational basis, which can only affect relative phases, thereby rendering it incapable of generating or transporting entanglement.

Discussion and conclusion—In this Letter, we systematically investigate entanglement dynamics across diverse quantum systems, moving beyond the conventional focus on product states to explore initial states that already possess entanglement. Our central finding is a universal three-class classification of entanglement growth. Most notably, we uncover a nonmonotonic dependence of HCEE increase on initial entanglement in MBL dynamics (we also considered the quantum sun model [120], more consistent results are detailed in SM [91]) and specific RQCs—a behavior qualitatively distinct from thermal dynamics. To fundamentally account for these novel results, we introduce the "build-move" framework. This framework offers a universal lens through which to understand complex entanglement growth by classifying dynamics based on their capacity to generate new entanglement ("build") and effectively transport preexisting entanglement ("move").

Our Letter yields another key insight by distinguishing between the entanglement of a single, fixed bipartition (HCEE) and the overall inherent entanglement in the quantum state, which we quantify using the BAEE. Figure 3 illustrates that, even in a generic thermalized system, the BAEE grows considerably faster than the HCEE during early dynamics. This initial divergence quantifies the rapid buildup of entanglement throughout the system at a local level, effectively establishing an accumulating intrasubsystem entanglement reservoir. This reservoir is central to understanding the initial increase of ΔS with S_{initial} in move-dominated dynamics: a larger reservoir provides more entanglement potential to be "moved" across the central bond. Our results demonstrate that MBL dynamics effectively unlock this potential, converting the hidden reservoir $\bar{S} - S$ into accessible half-chain entropy via the "move" mechanism. This picture is supported by a remarkable quantitative consistency: the value of S_{initial} where the entropy growth ΔS peaks for MBL dynamics [Fig. 1(d)] aligns with the maximum difference between BAEE and HCEE. This alignment provides compelling evidence for the dominant "move" mechanism in MBL entanglement dynamics, fundamentally recasting MBL as a global redistributor of a "hidden" entanglement reservoir.

This perspective underscores the limitation of using a single bipartition's EE to fully capture a system's entanglement structure and highlights the importance of multipartition entanglement measures, a topic of growing interest [121–123]. Our Letter provides a clear dynamical context for this multipartition viewpoint. Moreover, the distinct dynamical signatures predicted by our framework present clear targets for experimental verification on near-term quantum simulation platforms. Finally, our results have practical significance for numerical approaches: the saturation entanglement of MBL dynamics, which is reached only after exponentially long timescales, can be effectively approximated by the BAEE or random SWAP circuits. This provides a basis for utilizing efficient proxies to estimate steady-state properties while bypassing the prohibitive computational cost of simulating the full dynamical evolution.

Acknowledgments—C.-Y. Z. and Z.-X. L. are supported by Beijing Natural Science Foundation (No. F251001), the National Natural Science Foundation of China (No. 12347107 and No. 12474146), and the New Cornerstone Investigator Program. S.-X. Z. acknowledges the support from Quantum Science and Technology-National Science and Technology Major Project (No. 2024ZD0301700), the National Natural Science Foundation of China (No. 12574546), and the Chinese Academy of Sciences (No. XDB1680201 and No. YSBR-150).

Data availability—The data that support the findings of this article are openly available [124].

[1] O. Gühne and G. Tóth, Entanglement detection, Phys. Rep. **474**, 1 (2009).
[2] M. A. Nielsen and I. L. Chuang, *Quantum Computation and Quantum Information* (Cambridge University Press, Cambridge, England, 2010).
[3] R. Horodecki, P. Horodecki, M. Horodecki, and K. Horodecki, Quantum entanglement, Rev. Mod. Phys. **81**, 865 (2009).
[4] A. M. Kaufman, M. E. Tai, A. Lukin, M. Rispoli, R. Schittko, P. M. Preiss, and M. Greiner, Quantum thermalization through entanglement in an isolated many-body system, Science **353**, 794 (2016).
[5] P. Calabrese and J. Cardy, Entanglement entropy and quantum field theory, J. Stat. Mech. (2004) P06002.
[6] C. H. Bennett, H. J. Bernstein, S. Popescu, and B. Schumacher, Concentrating partial entanglement by local operations, Phys. Rev. A **53**, 2046 (1996).
[7] T. Zhou and D. J. Luitz, Operator entanglement entropy of the time evolution operator in chaotic systems, Phys. Rev. B **95**, 094206 (2017).
[8] J. Eisert, M. Cramer, and M. B. Plenio, Colloquium: Area laws for the entanglement entropy, Rev. Mod. Phys. **82**, 277 (2010).
[9] T. Nishioka, Entanglement entropy: Holography and renormalization group, Rev. Mod. Phys. **90**, 035007 (2018).
[10] D. Toniolo and S. Bose, Dynamical α-Rényi entropies of local Hamiltonians grow at most linearly in time, Phys. Rev. X **15**, 031046 (2025).
[11] E. Bianchi, L. Hackl, and N. Yokomizo, Linear growth of the entanglement entropy and the Kolmogorov-Sinai rate, J. High Energy Phys. 03 (2018) 25.

[12] Y. Han and X. Chen, Entanglement dynamics in U(1) symmetric hybrid quantum automaton circuits, Quantum **7**, 1200 (2023).

[13] M. Mezei and D. Stanford, On entanglement spreading in chaotic systems, J. High Energy Phys. 05 (2017) 65.

[14] J. M. Deutsch, Quantum statistical mechanics in a closed system, Phys. Rev. A **43**, 2046 (1991).

[15] T. Zhou and A. Nahum, Emergent statistical mechanics of entanglement in random unitary circuits, Phys. Rev. B **99**, 174205 (2019).

[16] M. Srednicki, Chaos and quantum thermalization, Phys. Rev. E **50**, 888 (1994).

[17] R. Oliveira, O. C. O. Dahlsten, and M. B. Plenio, Generic entanglement can be generated efficiently, Phys. Rev. Lett. **98**, 130502 (2007).

[18] A. Hamma, S. Santra, and P. Zanardi, Quantum entanglement in random physical states, Phys. Rev. Lett. **109**, 040502 (2012).

[19] H. Kim and D. A. Huse, Ballistic spreading of entanglement in a diffusive nonintegrable system, Phys. Rev. Lett. **111**, 127205 (2013).

[20] T. Rakovszky, F. Pollmann, and C. W. von Keyserlingk, Sub-ballistic growth of Rényi entropies due to diffusion, Phys. Rev. Lett. **122**, 250602 (2019).

[21] A. Nahum, J. Ruhman, S. Vijay, and J. Haah, Quantum entanglement growth under random unitary dynamics, Phys. Rev. X **7**, 031016 (2017).

[22] C. W. von Keyserlingk, T. Rakovszky, F. Pollmann, and S. L. Sondhi, Operator hydrodynamics, OTOCs, and entanglement growth in systems without conservation laws, Phys. Rev. X **8**, 021013 (2018).

[23] A. Nahum, S. Vijay, and J. Haah, Operator spreading in random unitary circuits, Phys. Rev. X **8**, 021014 (2018).

[24] B. Bertini, P. Kos, and T. c. v. Prosen, Entanglement spreading in a minimal model of maximal many-body quantum chaos, Phys. Rev. X **9**, 021033 (2019).

[25] M. Rigol, V. Dunjko, and M. Olshanii, Thermalization and its mechanism for generic isolated quantum systems, Nature (London) **452**, 854 (2008).

[26] A. Russotto, F. Ares, and P. Calabrese, Symmetry breaking in chaotic many-body quantum systems at finite temperature, Phys. Rev. E **112**, L032101 (2025).

[27] D. Basko, I. Aleiner, and B. Altshuler, Metal–insulator transition in a weakly interacting many-electron system with localized single-particle states, Ann. Phys. (Amsterdam) **321**, 1126 (2006).

[28] M. Žnidarič, T. c. v. Prosen, and P. Prelovšek, Many-body localization in the Heisenberg *xxz* magnet in a random field, Phys. Rev. B **77**, 064426 (2008).

[29] A. Pal and D. A. Huse, Many-body localization phase transition, Phys. Rev. B **82**, 174411 (2010).

[30] R. Vosk and E. Altman, Many-body localization in one dimension as a dynamical renormalization group fixed point, Phys. Rev. Lett. **110**, 067204 (2013).

[31] M. Serbyn, Z. Papić, and D. A. Abanin, Local conservation laws and the structure of the many-body localized states, Phys. Rev. Lett. **111**, 127201 (2013).

[32] D. A. Huse, R. Nandkishore, and V. Oganesyan, Phenomenology of fully many-body-localized systems, Phys. Rev. B **90**, 174202 (2014).

[33] E. Altman and R. Vosk, Universal dynamics and renormalization in many-body-localized systems, Annu. Rev. Condens. Matter Phys. **6**, 383 (2015).

[34] S. Campbell, M. J. M. Power, and G. De Chiara, Dynamics and asymptotics of correlations in a many-body localized system, Eur. Phys. J. D **71**, 206 (2017).

[35] M. Schreiber, S. S. Hodgman, P. Bordia, H. P. Lüschen, M. H. Fischer, R. Vosk, E. Altman, U. Schneider, and I. Bloch, Observation of many-body localization of interacting fermions in a quasirandom optical lattice, Science **349**, 842 (2015).

[36] J. yoon Choi, S. Hild, J. Zeiher, P. Schauß, A. Rubio-Abadal, T. Yefsah, V. Khemani, D. A. Huse, I. Bloch, and C. Gross, Exploring the many-body localization transition in two dimensions, Science **352**, 1547 (2016).

[37] A. Lukin, M. Rispoli, R. Schittko, M. E. Tai, A. M. Kaufman, S. Choi, V. Khemani, J. Léonard, and M. Greiner, Probing entanglement in a many-body–localized system, Science **364**, 256 (2019).

[38] R. Fan, P. Zhang, H. Shen, and H. Zhai, Out-of-time-order correlation for many-body localization, Sci. Bull. **62**, 707 (2017).

[39] Y. Huang, Y.-L. Zhang, and X. Chen, Out-of-time-ordered correlators in many-body localized systems, Ann. Phys. (Amsterdam) **529**, 1600318 (2017).

[40] X. Chen, T. Zhou, D. A. Huse, and E. Fradkin, Out-of-time-order correlations in many-body localized and thermal phases, Ann. Phys. (Amsterdam) **529**, 1600332 (2017).

[41] S. Liu, H.-K. Zhang, S. Yin, S.-X. Zhang, and H. Yao, Quantum Mpemba effects in many-body localization systems, Sci. Bull. **70**, 3991 (2025).

[42] R. Nandkishore and D. A. Huse, Many-body localization and thermalization in quantum statistical mechanics, Annu. Rev. Condens. Matter Phys. **6**, 15 (2015).

[43] R. Vasseur, S. A. Parameswaran, and J. E. Moore, Quantum revivals and many-body localization, Phys. Rev. B **91**, 140202(R) (2015).

[44] D. J. Luitz, N. Laflorencie, and F. Alet, Extended slow dynamical regime close to the many-body localization transition, Phys. Rev. B **93**, 060201(R) (2016).

[45] F. Iemini, A. Russomanno, D. Rossini, A. Scardicchio, and R. Fazio, Signatures of many-body localization in the dynamics of two-site entanglement, Phys. Rev. B **94**, 214206 (2016).

[46] T. Enss, F. Andraschko, and J. Sirker, Many-body localization in infinite chains, Phys. Rev. B **95**, 045121 (2017).

[47] R.-Q. He and Z.-Y. Lu, Characterizing many-body localization by out-of-time-ordered correlation, Phys. Rev. B **95**, 054201 (2017).

[48] K. Slagle, Z. Bi, Y.-Z. You, and C. Xu, Out-of-time-order correlation in marginal many-body localized systems, Phys. Rev. B **95**, 165136 (2017).

[49] M. Žnidarič, Entanglement in a dephasing model and many-body localization, Phys. Rev. B **97**, 214202 (2018).

[50] J. Zakrzewski and D. Delande, Spin-charge separation and many-body localization, Phys. Rev. B **98**, 014203 (2018).

[51] J. Sirker, Exploration of the existence of a distinct quasi many-body localized phase: Numerical study of a translationally invariant system in the thermodynamic limit, Phys. Rev. B **99**, 075162 (2019).

[52] J. Lee, D. Kim, and D.-H. Kim, Typical growth behavior of the out-of-time-ordered commutator in many-body localized systems, Phys. Rev. B **99**, 184202 (2019).

[53] T. Chanda, P. Sierant, and J. Zakrzewski, Time dynamics with matrix product states: Many-body localization transition of large systems revisited, Phys. Rev. B **101**, 035148 (2020).

[54] P. Sierant and J. Zakrzewski, Challenges to observation of many-body localization, Phys. Rev. B **105**, 224203 (2022).

[55] M. Serbyn, M. Knap, S. Gopalakrishnan, Z. Papić, N. Y. Yao, C. R. Laumann, D. A. Abanin, M. D. Lukin, and E. A. Demler, Interferometric probes of many-body localization, Phys. Rev. Lett. **113**, 147204 (2014).

[56] F. Andraschko, T. Enss, and J. Sirker, Purification and many-body localization in cold atomic gases, Phys. Rev. Lett. **113**, 217201 (2014).

[57] P. Ponte, Z. Papić, F. Huveneers, and D. A. Abanin, Many-body localization in periodically driven systems, Phys. Rev. Lett. **114**, 140401 (2015).

[58] S.-X. Zhang and H. Yao, Universal properties of many-body localization transitions in quasiperiodic systems, Phys. Rev. Lett. **121**, 206601 (2018).

[59] R. Vosk, D. A. Huse, and E. Altman, Theory of the many-body localization transition in one-dimensional systems, Phys. Rev. X **5**, 031032 (2015).

[60] D. A. Abanin, E. Altman, I. Bloch, and M. Serbyn, Colloquium: Many-body localization, thermalization, and entanglement, Rev. Mod. Phys. **91**, 021001 (2019).

[61] P. Sierant, M. Lewenstein, A. Scardicchio, L. Vidmar, and J. Zakrzewski, Many-body localization in the age of classical computing, Rep. Prog. Phys. **88**, 026502 (2025).

[62] J. Smith, A. Lee, P. Richerme, B. Neyenhuis, P. W. Hess, P. Hauke, M. Heyl, D. A. Huse, and C. Monroe, Many-body localization in a quantum simulator with programmable random disorder, Nat. Phys. **12**, 907 (2016).

[63] R. Vasseur and J. E. Moore, Nonequilibrium quantum dynamics and transport: From integrability to many-body localization, J. Stat. Mech. (2016) P064010.

[64] Y. Zeng, A. Hamma, Y.-R. Zhang, Q. Liu, R. Li, H. Fan, and W.-M. Liu, Logarithmic light cone, slow entanglement growth, and quantum memory, Phys. Rev. B **112**, 094202 (2025).

[65] Y. Chen, Universal logarithmic scrambling in many body localization, arXiv:1608.02765.

[66] I. H. Kim, A. Chandran, and D. A. Abanin, Local integrals of motion and the logarithmic lightcone in many-body localized systems, arXiv:1412.3073.

[67] A. Nanduri, H. Kim, and D. A. Huse, Entanglement spreading in a many-body localized system, Phys. Rev. B **90**, 064201 (2014).

[68] D.-L. Deng, X. Li, J. H. Pixley, Y.-L. Wu, and S. Das Sarma, Logarithmic entanglement lightcone in many-body localized systems, Phys. Rev. B **95**, 024202 (2017).

[69] I. MacCormack, M. T. Tan, J. Kudler-Flam, and S. Ryu, Operator and entanglement growth in nonthermalizing systems: Many-body localization and the random singlet phase, Phys. Rev. B **104**, 214202 (2021).

[70] J. H. Bardarson, F. Pollmann, and J. E. Moore, Unbounded growth of entanglement in models of many-body localization, Phys. Rev. Lett. **109**, 017202 (2012).

[71] M. Serbyn, Z. Papić, and D. A. Abanin, Universal slow growth of entanglement in interacting strongly disordered systems, Phys. Rev. Lett. **110**, 260601 (2013).

[72] D. Toniolo and S. Bose, Dynamics of many-body localized systems: Logarithmic lightcones and log t-law of α-Rényi entropies, arXiv:2408.02016.

[73] P. Calabrese and J. Cardy, Evolution of entanglement entropy in one-dimensional systems, J. Stat. Mech. (2005) P04010.

[74] P. Calabrese and J. Cardy, Quantum quenches in extended systems, J. Stat. Mech. (2007) P06008.

[75] K. Kawabata, T. Numasawa, and S. Ryu, Entanglement phase transition induced by the non-Hermitian skin effect, Phys. Rev. X **13**, 021007 (2023).

[76] X. Feng, S. Liu, S.-X. Zhang, and S. Chen, Numerical instability of non-Hermitian Hamiltonian evolution, Phys. Rev. B **111**, 224310 (2025).

[77] S. Guo, S. Yin, S.-X. Zhang, and Z.-X. Li, Skin effect induced anomalous dynamics from charge-fluctuating initial states, Phys. Rev. B **112**, 155419 (2025).

[78] P. W. Anderson, Absence of diffusion in certain random lattices, Phys. Rev. **109**, 1492 (1958).

[79] J. Billy, V. Josse, Z. Zuo, A. Bernard, B. Hambrecht, P. Lugan, D. Clément, L. Sanchez-Palencia, P. Bouyer, and A. Aspect, Direct observation of Anderson localization of matter waves in a controlled disorder, Nature (London) **453**, 891 (2008).

[80] B. Kramer and A. MacKinnon, Localization: Theory and experiment, Rep. Prog. Phys. **56**, 1469 (1993).

[81] D. Vollhardt and P. Wölfle, Diagrammatic, self-consistent treatment of the anderson localization problem in $d \leq 2$ dimensions, Phys. Rev. B **22**, 4666 (1980).

[82] T. Giamarchi and H. J. Schulz, Anderson localization and interactions in one-dimensional metals, Phys. Rev. B **37**, 325 (1988).

[83] E. Tarquini, G. Biroli, and M. Tarzia, Critical properties of the anderson localization transition and the high-dimensional limit, Phys. Rev. B **95**, 094204 (2017).

[84] I. V. Gornyi, A. D. Mirlin, and D. G. Polyakov, Interacting electrons in disordered wires: Anderson localization and low-t transport, Phys. Rev. Lett. **95**, 206603 (2005).

[85] A. De Luca, B. L. Altshuler, V. E. Kravtsov, and A. Scardicchio, Anderson localization on the Bethe lattice: Nonergodicity of extended states, Phys. Rev. Lett. **113**, 046806 (2014).

[86] Y. Qing, Y.-Q. Chen, and S.-X. Zhang, Entanglement growth and information capacity in a quasiperiodic system with a single-particle mobility edge, Phys. Rev. B **113**, 064308 (2025).

[87] P. A. Lee and T. V. Ramakrishnan, Disordered electronic systems, Rev. Mod. Phys. **57**, 287 (1985).

[88] F. Evers and A. D. Mirlin, Anderson transitions, Rev. Mod. Phys. **80**, 1355 (2008).

[89] G. Roati, C. D'Errico, L. Fallani, M. Fattori, C. Fort, M. Zaccanti, G. Modugno, M. Modugno, and M. Inguscio, Anderson localization of a non-interacting Bose–Einstein condensate, Nature (London) **453**, 895 (2008).

[90] K. Tikhonov and A. Mirlin, From anderson localization on random regular graphs to many-body localization, Ann. Phys. (Amsterdam) **435**, 168525 (2021).

[91] See Supplemental Material at http://link.aps.org/supplemental/10.1103/xkh7-gdqm for numerical details; level spacing analysis; analytical proofs regarding the random SWAP circuit; extended analyses of various initial states and BAEE; and robustness and universality tests including the quantum sun model, integrable chains, and dual-unitary circuits, which includes Refs. [92–101].

[92] V. Oganesyan and D. A. Huse, Localization of interacting fermions at high temperature, Phys. Rev. B **75**, 155111 (2007).

[93] P. Roushan *et al.*, Spectroscopic signatures of localization with interacting photons in superconducting qubits, Science **358**, 1175 (2017).

[94] O. Bohigas, M. J. Giannoni, and C. Schmit, Characterization of chaotic quantum spectra and universality of level fluctuation laws, Phys. Rev. Lett. **52**, 1 (1984).

[95] M. L. Mehta, *Random Matrices* (Elsevier, New York, 2004).

[96] Y. Y. Atas, E. Bogomolny, O. Giraud, and G. Roux, Distribution of the ratio of consecutive level spacings in random matrix ensembles, Phys. Rev. Lett. **110**, 084101 (2013).

[97] C.-Y. Zhang, S.-X. Zhang, and Z.-X. Li, Bond additivity and persistent geometric imprints of entanglement in quantum thermalization, arXiv:2601.01327.

[98] B. Bertini, P. Kos, and T. c. v. Prosen, Exact correlation functions for dual-unitary lattice models in $1+1$ dimensions, Phys. Rev. Lett. **123**, 210601 (2019).

[99] S. A. Rather, S. Aravinda, and A. Lakshminarayan, Creating ensembles of dual unitary and maximally entangling quantum evolutions, Phys. Rev. Lett. **125**, 070501 (2020).

[100] B. Bertini, P. Kos, and T. Prosen, Operator entanglement in local quantum circuits I: Chaotic dual-unitary circuits, SciPost Phys. **8**, 067 (2020).

[101] L. Piroli, B. Bertini, J. I. Cirac, and T. c. v. Prosen, Exact dynamics in dual-unitary quantum circuits, Phys. Rev. B **101**, 094304 (2020).

[102] Y.-Q. Chen, S. Liu, and S.-X. Zhang, Subsystem information capacity in random circuits and Hamiltonian dynamics, Quantum **9**, 1783 (2025).

[103] M. P. Fisher, V. Khemani, A. Nahum, and S. Vijay, Random quantum circuits, Annu. Rev. Condens. Matter Phys. **14**, 335 (2023).

[104] M. Žnidarič, Exact convergence times for generation of random bipartite entanglement, Phys. Rev. A **78**, 032324 (2008).

[105] Y. Li, X. Chen, and Matthew P. A. Fisher, Quantum Zeno effect and the many-body entanglement transition, Phys. Rev. B **98**, 205136 (2018).

[106] Y. Li, X. Chen, and Matthew P. A. Fisher, Measurement-driven entanglement transition in hybrid quantum circuits, Phys. Rev. B **100**, 134306 (2019).

[107] S. Liu, M.-R. Li, S.-X. Zhang, S.-K. Jian, and H. Yao, Universal Kardar-Parisi-Zhang scaling in noisy hybrid quantum circuits, Phys. Rev. B **107**, L201113 (2023).

[108] S. Liu, M.-R. Li, S.-X. Zhang, S.-K. Jian, and H. Yao, Noise-induced phase transitions in hybrid quantum circuits, Phys. Rev. B **110**, 064323 (2024).

[109] S. Liu, M.-R. Li, S.-X. Zhang, and S.-K. Jian, Entanglement structure and information protection in noisy hybrid quantum circuits, Phys. Rev. Lett. **132**, 240402 (2024).

[110] S. Liu, H.-K. Zhang, S. Yin, and S.-X. Zhang, Symmetry restoration and quantum Mpemba effect in symmetric random circuits, Phys. Rev. Lett. **133**, 140405 (2024).

[111] B. Skinner, J. Ruhman, and A. Nahum, Measurement-induced phase transitions in the dynamics of entanglement, Phys. Rev. X **9**, 031009 (2019).

[112] A. Lerose, M. Sonner, and D. A. Abanin, Influence matrix approach to many-body Floquet dynamics, Phys. Rev. X **11**, 021040 (2021).

[113] W. Wang, S. Liu, J. Li, S.-X. Zhang, and S. Yin, Driven critical dynamics in measurement-induced phase transitions, arXiv:2411.06648.

[114] K. Chalas, P. Calabrese, and C. Rylands, Quench dynamics of entanglement from crosscap states, SciPost Phys. **19**, 132 (2025).

[115] R. Patil, L. Hackl, G. R. Fagan, and M. Rigol, Average pure-state entanglement entropy in spin systems with SU(2) symmetry, Phys. Rev. B **108**, 245101 (2023).

[116] E. Bianchi and P. Donà, Typical entanglement entropy in the presence of a center: Page curve and its variance, Phys. Rev. D **100**, 105010 (2019).

[117] P. Vivo, M. P. Pato, and G. Oshanin, Random pure states: Quantifying bipartite entanglement beyond the linear statistics, Phys. Rev. E **93**, 052106 (2016).

[118] D. N. Page, Average entropy of a subsystem, Phys. Rev. Lett. **71**, 1291 (1993).

[119] Y. Lu, P. Shi, X.-H. Wang, J. Hu, and S.-J. Ran, Persistent ballistic entanglement spreading with optimal control in quantum spin chains, Phys. Rev. Lett. **133**, 070402 (2024).

[120] J. Šuntajs and L. Vidmar, Ergodicity breaking transition in zero dimensions, Phys. Rev. Lett. **129**, 060602 (2022).

[121] S. Singha Roy, S. N. Santalla, J. Rodríguez-Laguna, and G. Sierra, Entanglement as geometry and flow, Phys. Rev. B **101**, 195134 (2020).

[122] A. A. Akhtar and Y.-Z. You, Multiregion entanglement in locally scrambled quantum dynamics, Phys. Rev. B **102**, 134203 (2020).

[123] D. Kolisnyk, R. A. Medina, R. Vasseur, and M. Serbyn, Tensor cross interpolation of purities in quantum many-body systems, Quantum **10**, 2114 (2026).

[124] C.-Y. Zhang, Z.-X. Li, and S.-X. Zhang, GitHub (2026), https://github.com/Chunyue-Zhang/Entanglement-Growth-from-Entangled-States.